Biogeosciences Discuss., 11, 13699–13737, 2014
www.biogeosciences-discuss.net/11/13699/2014/
doi:10.5194/bgd-11-13699-2014

Biogeosciences Discussions
Open Access

Quantitative estimation and vertical partitioning of the soil carbon dioxide fluxes at the hillslope scale on a loess soil

F. Wiaux[1], **K. Van Oost**[2,3], **and M. Vanclooster**[1]

[1]Environmental Sciences, Earth & Life Institute, Université catholique de Louvain, Croix du Sud 2, 1348 Louvain-la-Neuve, Belgium
[2]George Lemaître Centre for Earth and Climate Research, Earth & Life Institute, Université catholique de Louvain, Place Louis Pasteur 3, 1348 Louvain-la-Neuve, Belgium
[3]Fonds National pour la Recherche Scientifique (FNRS), Belgium

Received: 6 August 2014 – Accepted: 31 August 2014 – Published: 22 September 2014

Correspondence to: F. Wiaux (francois.wiaux@uclouvain.be)

Published by Copernicus Publications on behalf of the European Geosciences Union.

Abstract

Both modelling and experimental approaches have been applied to assess C exchange fluxes at large spatial scales. Yet, these approaches are subjected to substantial limitations and uncertainties. Here, we aim to highlight two key mechanisms able to improve the estimation of the hillslope aggregated CO_2 fluxes: (i) the persistence of soil organic carbon (OC) in deep colluvium deposits; and (ii) the physical controls on CO_2 fluxes along soil profiles. This study focuses on a sloping cropland in the central loess belt of Belgium. On two contrasted soil types along the studied hillslope, we recorded time-series of CO_2 concentration, water content and temperature along 1 m long soil profiles during two periods of 6 months. Then, we calculated profiles of CO_2 fluxes using the gradient method. To extrapolate these fluxes to entire yearly periods (2011–2013), we performed simulation using the SOILCO$_2$RothC model.

The vertical partitioning of the soil CO_2 fluxes shows that ca. 90 to ca. 95 % of the surface CO_2 fluxes originates from the 10 first centimeters of the soil profile at the footslope. We show that high water filled pore space at this slope position disables the transfer of biotic CO_2 along the soil profile. However, the total annual flux averaged along 3 years of simulation show that the top soil layer (0–10 cm) of the footslope generates CO_2 fluxes (870 ± 64 CO_2-C m^{-2} $year^{-1}$) which exceed those observed at the summit position (583 ± 61 CO_2-C m^{-2} $year^{-1}$). Hence, our results reconcile two seemingly contradictory hypotheses, i.e. (i) these support that soil OC at such a footslope is stored along the main part of the soil profile and submitted to a long-term stabilization, and (ii) at the same time these support that the depositional footslope profile emits more CO_2 than the summit, due to its high amount and quality of OC. Our results support the need to consider slopes when modeling soil-atmosphere C exchanges. If landscapes dynamic processes are not accounted for, we pointed out a risk to underestimate annual soil-atmosphere CO_2 exchanges by ca. 20 %.

BGD
11, 13699–13737, 2014

1 Introduction

Soils play a major role in the global C budget, as they contain 2 to 3 times more C than the atmosphere and ca. 3 times more C than the aboveground biomass. In addition, the size of soil C pool corresponds approximately to a third of the geological reservoir present as fossil fuels (Eswaran et al., 1993; Lal et al., 2003).

Current large scale estimations of the exchange of C between the soil and the atmosphere are associated with large uncertainties (Houghton et al., 2003, 2007; Peters et al., 2010). Both modelling and experimental approaches have been applied to assess C exchange fluxes at large spatial scales. Yet these approaches are subjected to substantial limitations: (i) the current technical possibilities to measure directly hillslope aggregated CO_2 fluxes are limited (e.g. Baldocchi, 2003), and (ii) the complexity of processes at the scale of a whole catchment is not fully considered in current models of C at the soil-atmosphere interface (Chaopricha and Marín-Spiotta, 2014; Trumbore and Czimczik, 2008).

In-situ measurements of the hillslope aggregated CO_2 fluxes has been largely achieved using the Eddy-Covariance technique (e.g. Goulden et al., 1996; Eugster et al., 2010), but this technique is not appropriate for sloping landscapes, providing an uncertainty on the CO_2 fluxes ranging from 100 to 200 g C m^{-2} $year^{-1}$ at such non-ideal sites (Baldocchi, 2003). At the local scale, more precise technologies such as survey chambers with infra-red gas analyzers (IRGA) (e.g. Davidson et al., 2002) or such as the non-dispersive infra-red (NDIR) probes (e.g. Young et al., 2009) can be used. However the support scale and spatial resolution of these devices are often too small to make robust large scale assessment of C exchanges across the soil atmosphere interface.

Alternatively, soil modeling of OC dynamics allows assessing the heterotrophic soil respiration (e.g. Herbst et al., 2008). Such models simulations have already been used to calculate the hillslope aggregated CO_2 fluxes (e.g. Dai et al., 2012). However, the predictive capabilities of the models are limited because they do not account for the

BGD
11, 13699–13737, 2014

varying topography and biophysical conditions across the landscape (Dai et al., 2012), and because some key mechanisms controlling the soil CO_2 efflux are not sufficiently implemented in current OC dynamic models: (i) the physical controls on CO_2 fluxes, e.g. gas diffusion barriers along soil profiles, (e.g. Ball, 2013; Maier et al., 2011; Wiaux et al, 2014c); and (ii) the contribution of buried OC at downslope depositional areas to soil C emissions (e.g. Van Oost et al., 2012; Wang et al., 2014; Wiaux et al., 2014a).

While the transfer of soil OC by erosion has been recognized (e.g. Quinton et al., 2010; Stallard, 1998), its impact on both local and global C budgets is poorly understood (Lal, 2003), and consequently not implemented in OC dynamics models. Once brought at the bottom of the slope, sediments deposits enriched in soil OC accumulate and are progressively buried deeper and deeper along the soil profiles, forming colluvic soils at the depositional site, with an increasing soil OC stock (Van Oost et al. 2005a, b, 2012; Wiaux et al., 2014a). However, a series of complex and interacting processes are acting in these depositional sites, able to decrease as well to enhance mineralization (Lal, 2003; Wiaux et al., 2014b). Recent studies (Rumpel and Kögel-Knabner, 2011) highlighted that deep soil OC is highly processed, and showed the need to study more in details the C fluxes coming from deep soil horizons. Recently, through a vertical partitioning of CO_2 fluxes along soil profiles, some authors (Takahashi et al., 2004; Davidson et al., 2006; Goffin et al., 2014) showed that the 30 first centimeters of soil significantly contribute to the total surface CO_2 flux. However, to our knowledge, such a vertical partitioning has never been carried out neither in larger scale agro-ecosystems nor in downslope colluvium with buried OC in deep soil layers.

In this study, we aim to quantify the soil-atmosphere C flux at the scale of a hillslope. More specifically, we aim to evaluate two key mechanisms able to improve this estimation of the hillslope aggregated CO_2 fluxes: (i) the persistence of OC in deep colluvium deposits through a vertical partitioning of soil CO_2 fluxes; and (ii) the physical controls on CO_2 fluxes along soil profiles.

BGD
11, 13699–13737, 2014

2 Material and methods

2.1 Study site description

The study was carried out in the Belgian loam belt along a cultivated hillslope of 150 m length (50.6669° N, 4.6331° W). The site has a maritime temperate climate, with an average annual temperature of 9.7 °C and an average annual precipitation of 805 mm. The study site is described in detail in Wiaux et al. (2014a, b). We selected 2 measurement stations along the hillslope: one at the summit and one at the footslope position. The soil is a Dystric Luvisol type at the summit and a Colluvic Regosol in the depositional area at the footslope (Wiaux et al., 2014a, b). The soil properties of these two soil profiles have been characterized by Wiaux et al. (2014a, b): soil total OC, labile pool OC and porosity profiles are illustrated on Figs. 1 and 2, respectively.

The total porosity ($\emptyset$) was measured in the laboratory by weighting 100 cm^3 undisturbed soil cores both at saturation and after oven drying at 105 °C during 48 h. The $\emptyset$ was then deduced from the mass of water needed to fill sample pores. The air-filled porosity (ε) was calculated as the difference between $\emptyset$ and VWC. Average and standard deviation values were calculated on triplicate samples for each depth.

Soil water retention (SWR) curves were characterized using undisturbed soil cores at 10, 25, 35, 50, 70 and 95 cm depth, with 3 replicates at each depth. ε_{100} and b parameters were obtained by fitting the Campbell (1974) model of SWR curve to the SWR observations (Moldrup et al., 2000).

2.2 Monitoring of soil CO_2, water and temperature

We measured soil CO_2 concentrations by means of specific designed soil CO_2 probes. The CO_2 sensor in the probe is based on the CARBOCAP® Single-Beam Dual Wavelength non-dispersive infra-red (NDIR) technology (GMM221, Vaisala corp., Vantaa, Finland). Analytical precision is 1.5 % of the measurement range added to 2 % of the observed value. The sensor was covered with nylon and PTFE (polytetrafluoroethy-

BGD
11, 13699–13737, 2014

lene) membranes and encapsulated in a tube to avoid soil particles entering the sensor and to limit water infiltration. This tubing method is an adaptation of the technique presented by Young et al. (2009). These tubes were inserted vertically into the soil, after augering holes with a diameter that equals the diameter of the PVC tubes. To obtain an equilibrated soil environment around the soil concentration probe, we started measurements 1 month after the probes installation. The measurement plots were covered with a synthetic permeable geotextile during the complete measurement period (Fig. 4). This avoided vegetation growth and any autotrophic contribution to the soil respiration.

At each of the 2 slope positions, we measured soil CO_2 concentrations profiles at 4 soil depths with 3 replicates on each depth (Fig. 4). Triplicate CO_2 concentrations data were averaged, providing unique values for each depth, representative of the entire slope position. Continuous CO_2 concentrations profiles were generated by fitting a decreasing double sigmoidal model to the observations (Sect. 2.3).

As a reference, we performed surface CO_2 fluxes measurements with an infra-red gas analyzer (IRGA) linked to a survey chamber at 16 dates (profile and surface data matched in time, with a maximum time-lapse of 30 min between each other). The replicates of CO_2 concentration along soil profiles allowed catching its spatial variability at the different depths (Maier and Schack-Kirchner, 2014), extending the measurement footprint to the same area (i.e. 5 m^2) than the IRGA chamber network located at the soil surface (Fig. 4). These reference surface CO_2 fluxes allowed calibrating parameters of Eqs. (1) and (4) to ensure the accuracy of profile CO_2 fluxes (Sect. 2.3).

Soil temperature was monitored using a thermistor probe (Therm107, Campbell Scientific Lt., UK). Analytical precision is 0.4 °C. Soil volumetric water content (VWC) was monitored using Time Domain Reflectrometry (TDR) probes. Topp's equation (Topp et al., 1980) was used to determine VWC, from the apparent dielectric constant measured by TDR probes, as further described in Wiaux et al. (2014c).

Water, temperature and CO_2 concentration profiles measurements were recorded with an automatic data logger (CR1000, Campbell Scientific Lt., UK), connected to a multiplexer (AM16/32, Campbell Scientific, Campbell Scientific Lt., UK).

BGD
11, 13699–13737, 2014

At each of the 2 slope positions, we measured soil CO_2 concentrations profiles at 4 soil depths with 3 replicates at each depth (Fig. 4). Vaisala CO_2 probe concentrations ranges were adapted to each soil depth and to each slope position. This allowed to characterize the entire range of values without impacting the quality of observation in terms of precision. At the summit position, measurements ranged between 0–2 % at 12, 25, 45 cm depth and between 0–5 % at 85 cm depth. At the footslope position, measurement ranged between 0–5 % at 12 cm depth, between 0–10 % at 25 and 45 cm depth and between 0–20 % at 85 cm depth.

For soil VWC profiles, at each of the 2 slope positions, 18 measurements were collected (6 soil depths, 3 replicates). Sampling depths for VWC were 10, 25, 35, 50, 70 and 95 cm (Fig. 4). For temperature, 4 soil depths (10, 25, 45, 85 cm) without replicates were measured (Fig. 4).

Hourly time-series measurements of VWC, temperature and CO_2 concentration along soil profiles were performed in 2012 from 12 May to 13 December at the footslope and from 2 June until 13 December at the summit, and in 2013 from 14 May at the summit and 14 June 2013 at the footslope until 22 November 2013 at the two stations. In 2012, some CO_2 measurements were not always possible due to sensors failures and unsuitable measurement range of some sensors.

2.3 Calculation of the CO_2 fluxes

The flux of CO_2 was calculated using Fick's first law of diffusion according to the gradient method (Eq. 1, e.g. Maier and Schack-Kirchner, 2014).

$$F_{CO_2} = -D_s \frac{\partial CO_2}{\partial z} \quad (1)$$

where F_{CO_2} is the soil CO_2 flux [µmol m^{-2} s^{-1}], D_s the diffusivity of CO_2 in soil [m^2 s^{-1}], CO_2 the soil CO_2 concentration [µmol m^{-3}], and $\frac{\partial CO_2}{\partial z}$ the vertical soil CO_2 gradient.

In order to calculate the vertical soil CO_2 gradient, we used a double sigmoidal equation (Eq. 2), which allows accounting for some curve concavity variations (Wiaux et al.,

BGD
11, 13699–13737, 2014

2014c; Maier and Schack-Kirchner, 2014):

$$CO_2(z) = 0.04 + A\left(\left(\frac{1}{1+e^{-\gamma_1 z}}\right) + \left(\frac{1}{1+e^{-\gamma_2(z-d)}}\right) - \left(\frac{1}{2} + \frac{1}{e^{\gamma_2 d}+1}\right)\right) \quad (2)$$

where z is soil depth [cm], d is the soil depth [cm] at which the sharpness of the curve changes due to a diffusion barrier, γ_1 and γ_2 [cm^{-1}] are fitted parameters which characterize the sharpness of the curve, respectively above and below the soil depth d, and A [%] is a reference value used to define the fitted asymptotic value of the CO_2 concentration at infinite depth. The fitting parameters A, d, γ_1 and γ_2 were evaluated for each profile observation in time using a trust-region-reflective optimization algorithm in Matlab©. The derivative of this function (Eq. 2) provided the CO_2 gradient ($\frac{\partial CO_2}{\partial z}$) used in Eq. (1).

The diffusivity of CO_2 in soil (defined as D_s in Eq. 1) is a function of the diffusivity of CO_2 in free air (varying with temperature T and pressure, e.g. Davidson et al., 2006) and of the gas tortuosity factor (ξ) (Eq. 3).

$$D_s = \xi 1.47 \times 10^{-5}\left(\frac{T+273}{273}\right)^{1.75} \quad (3)$$

where ξ depends on soil physical and hydrological properties. We used the Moldrup et al. (2000) model (Eq. 4) which was shown to provide the most accurate and precise results (Davidson et al., 2006; Goffin et al., 2014; Wiaux et al., 2014c):

$$\xi = \left(2\varepsilon_{100}^3 + 0.04\varepsilon_{100}\right)\left(\frac{\varepsilon}{\varepsilon_{100}}\right)^{2+3/b} \quad (4)$$

where ε [$m^3\ m^{-3}$] is the soil air-filled porosity, b[−] is the slope of the Campbell (1974) soil water retention curve model between −100 and −500 cm H_2O water suction, and ε_{100} [$m^3\ m^{-3}$] is the soil air-filled porosity at a soil water potential of −100 cm H_2O.

BGD
11, 13699–13737, 2014

In contrast to other studies (e.g. Pingintha et al., 2010; Turcu et al., 2005), soil CO_2 diffusivity was not aggregated for the entire soil profile or for an entire soil layer, but its vertical distribution was accounted for Eq. (4) was inserted in Eq. (1), and Eq. (1) was numerically evaluated using a depth increment of 0.1 cm. The surface CO_2 flux obtained with the gradient-based method was considered as being the top of the calculated CO_2 flux profile using Eq. (1).

2.4 Data treatments and adjustments

To optimize the quality of the soil concentration data time-series, observations corresponding to battery voltage lower than 11.5 V were removed. Soil profile CO_2 concentrations measurements were a posteriori corrected for temperature variations using the empirical formulas described by Tang et al. (2003). This allowed removing the impact of temperature on the CO_2 reading of the CO_2 probe, since the CARBOCAP® technology is temperature dependent. Probe specific parameters values for these correction formulas were provided by the probe manufacturer (Vaisala corp., Vantaa, Finland).

Triplicate VWC and CO_2 concentrations data were averaged, providing unique values for each depth, representative of the entire slope position. Soil temperature and VWC profiles were calculated using a linear interpolation between the depth specific values. Surface values were not extrapolated, and were considered as being equal to the closest observations in the profiles. CO_2 concentrations profiles were generated by fitting a decreasing double sigmoidal model to the observations as described in the previous sub-section. The performance of this model (Eq. 2) was evaluated using the regression coefficient (R^2). When R^2 values of the fitted CO_2 profiles were lower than a threshold value of 95 %, the gradient of CO_2 concentration was considered as unreliable and CO_2 fluxes were not calculated at that time.

We calibrated the diffusion model by adjusting the parameters related to the gas diffusion coefficient (i.e. b and ε_{100} such that calculated fluxes fit punctual CO_2 fluxes observations. These observations were obtained by means of a portable infra-red gas analyzer with an automated closed dynamic chamber (LI-8100A system, LI-COR, United-

BGD
11, 13699–13737, 2014

States), following Davidson et al. (2002). The sampling design of these surface chamber CO_2 fluxes measurements on the same study site has been described in Wiaux et al. (2014 b). The regression coefficients of the relationship between both measured surface chamber and calculated CO_2 fluxes ensure the consistency (and consequently the precision) of the calculated fluxes (i.e. $R^2 = 92\,\%$ both in 2012 and 2013). The slope of the fit (i.e. 1.05 and 1.22, respectively in 2012 and 2013) was used to correct the calculated fluxes and to ensure accuracy, as explained in Wiaux et al. (2014c).

CO_2 fluxes, as assessed by the gradient based method, were calculated on an hourly time-scale, and then integrated on a daily basis. Temperature, VWC, diffusivity and CO_2 concentration values were so averaged on a daily basis.

2.5 Vertical partitioning of CO_2 fluxes

The space-continuous CO_2 fluxes profiles obtained using Eq. (2) were partitioned into 10 slides of 10 centimeters along the soil profile. For each soil slide, we calculated the difference between top and bottom fluxes. This difference was then divided by the total CO_2 flux (e.g. the value at the soil surface). This provides the relative contribution in terms of both CO_2 production and transfer (in %) of each soil slide to the surface CO_2 flux (e.g. Goffin et al., 2014; Maier and Schack-Kirchner, 2014).

In order to allow an easy representation of the temporal dynamic of this vertical partitioning, values were averaged on semi-seasonal time-scale. Standard deviation values reflect the variability in time during each semi-season.

2.6 Interpolation and aggregation of CO_2 fluxes in time and space

Field measurements were carried out during limited time periods, and hence would not allow assessing the C budget at the whole year scale. In order to obtain continuous time-series covering the entire yearly periods, an OC dynamics model was used as a tool to interpolate and extrapolate measured data of VWC, temperature and CO_2 fluxes for the period of 3 years (2011–2013). Then, we integrated the daily simulated

BGD
11, 13699–13737, 2014

CO_2 fluxes for each of the three studied years. These yearly CO_2 fluxes were averaged over the three studied years and compared between slope positions. The mean yearly CO_2 flux obtained at the summit position was considered to be representative of a non-sloping landscape. To calculate mean yearly CO_2 fluxes representative of a hilly landscape, we calculated a weighted average CO_2 flux of the summit and the footslope, thereby considering the fact that the footslope colluvium represents ca. 35 % of the surface area of the studied hillslope.

2.6.1 Description of the SoilCO_2-RothC model

The SoilCO_2-RothC model has been described in detail by Herbst et al. (2008). The model combines the coupling of a one-dimensional water, heat and CO_2 flux model (SOILCO_2) with a pool concept of carbon turnover (RothC) for the prediction of soil respiration. The performance of this model was previously evaluated by Herbst et al. (2008) based on a 8 years data set of CO_2 fluxes measurements, and its predictions were judged to be acceptable (with a difference of 0.007 g C m^{-2} d^{-1} between measured and simulated mean daily respiration rates).

This model was run on a daily time step for a period of three years (2011–2013), both for the summit and the footslope positions. Other temporal resolutions (i.e. hourly and weekly time steps) were evaluated but provided poor results.

The unsaturated soil water flux is described by the Richards equation, and both the soil water capacity and unsaturated hydraulic conductivity function are calculated according to Van Genuchten (1980). Heat transport is implemented according to Simunek and Suarez (1993). Transport of soil CO_2 is simulated considering diffusion and convection in the gas phase, as well as dispersion and convection in the liquid phase. For CO_2 diffusion in the gas phase, we implemented the new Moldrup et al. (2000) model (Eq. 4) which was shown to be appropriate for calculating CO_2 fluxes (Davidson et al., 2006; Goffin et al., 2014; Wiaux et al., 2014c).

For the production of CO_2, we only considered two different OC pools on the five ones allowed by the RothC model concept. First, all OC pools in our soils were sup-

BGD
11, 13699–13737, 2014

posed to participate to C dynamic processes, and hence the inert organic matter (IOM pool) was kept to zero. Then, we assumed the absence of both fresh and resistant plant material (DPM and RPM pools). Hence, the RPM pool was kept to zero, while the DPM pool, characterized by a high decomposition rate constant, was used to represent the labile OC pool (NaOCl-extracted OC, as defined in Sect. 3 for the soils studied here). As we did not discriminate here between primary (i.e. vegetal origin) and secondary (i.e. microbial origin) sources of OM, the biomass concentration (BIO pool) was supposed to be included in the labile OC pool, and hence kept to zero. The stable OC pool (NaOCl-resistant OC, as defined in Sect. 3 for the soils studied here) was represented in the RothC model by the humus pool (i.e. HUM) which has a low decomposition rate constant. Reduction factors functions are used to simulate the effect of CO_2 concentration, water pressure head, and temperature on the CO_2 production according to the original version of the SOILCO$_2$ model, as described by Simunek and Suarez (1993).

For the boundary conditions for the soil hydrological balance, we used meteorological data, i.e. precipitation and evapo-transpirationat at the top of the soil profiles, and a free drainage concept at the bottom of the soil profiles. Precipitations were directly measured in a meteorological station close to our study site (ca. 2 km). At the summit, we considered a run-off production once input water flux exceeds the infiltration capacity, while at the footslope we specified that water can accumulate at the soil surface. Daily evapo-transpiration was calculated according to the Penmann-Monteith equation, based on measured meteorological data. The boundary conditions of soil heat flow were defined using directly measured soil temperature both at the top and at the bottom of the soil profile.

2.6.2 Model parametrisation and calibration

In this study, 5 soil depth increments were considered for the two studied soil profiles, i.e. 0–18, 19–30, 31–45, 46–70, and 71–100 cm depth. These increments were chosen to consider the depths where measurements probes were installed and the soil structural properties (Wiaux et al., 2014a). The soil hydrodynamic parameters of the van

BGD
11, 13699–13737, 2014

Genuchten – Mualem function (Mualem, 1976; van Genuchten, 1980), as well as parameters related to the gas diffusion coefficients (i.e. b and ε_{100}) are specified for each soil material. The initial concentration of the labile and stable OC pools were specified for each soil material, as presented in Wiaux et al. (2014a).

For identifying the value of input parameters, we calibrated the model using the global inversion model PEST (e.g. Gallagher and Doherty, 2007). We used measured soil VWC, temperature and CO_2 concentration measurements, as well as calculated CO_2 fluxes within the profile to invert the model.

We carried out a simple sensitive analysis of the SOILCO$_2$-RothC model to identify key parameters. Among the more sensitive parameters, which could significantly impact the outputs of the model, we firstly inverted the 9 soil Mualem – van Genuchten parameters, related to VWC, both at the summit and at the footslope. In a second step, we kept them fixed and inverted parameters related to soil CO_2 fluxes, both at the summit and the footslope: (i) the 5 initial concentrations of the labile OC pool, (ii) the decomposition rate of the labile OC pool, (iii) the activation energy reflecting temperature sensitivity, as well as (iv) the HB1 coefficient (i.e. the value of the pressure head at which CO_2 production by soil micro-organisms is at the optimal level). Initial concentrations of the labile OC pool were inverted inside a realistic range of values (i.e. average ±3 times the standard deviation) as compared to the previous measurements done by Wiaux et al. (2014a). At the footslope, we additionally inverted the 5 ε_{100} parameters related to the gas diffusion.

3 Results

3.1 Spatio-temporal analysis of measured soil variables

Figure 5 shows the spatio-temporal variation of soil temperature, moisture and gas diffusion, and Fig. 6 shows the spatio-temporal variation of CO_2 concentrations and fluxes. All these values correspond to in-situ measurements during period of ca. 6

BGD
11, 13699–13737, 2014

months in 2013. Similar measurements have been carried out in 2012 and display similar spatio-temporal trends (data not shown).

The soil temperature (Fig. 5) does not significantly differ between the summit and the footslope, except during July (day of year 180 to 220) where temperatures are ca. 2 to 3° higher at the summit while they follow exactly the same temporal dynamic. The surface mean daily temperatures vary all along the soil profiles from 4 to 28 °C at the summit, and from 4 to 28 °C at the footslope (for the period of measurements).

The space-time dynamics of soil volumetric water content (VWC, Fig. 5) differ completely between the summit and the footslope. At the footslope, soil VWC values remained inside a narrow interval (36 to 39 %) all along the soil profile during the considered period. At the summit, soil VWC varies from 23 to 34 % in the plow layer (0–30 cm depth) and then increases by an absolute value of 15 to 5 % (respectively) in the rest of the soil profile. The soil at the summit position is the wettest during the early spring and the late autumn and driest in the summer. At the footslope soil VWC reaches the saturation level in the early summer after an important rainfall event and then slowly decreases until the early autumn and reaches saturation again in the late autumn. Similarly, in the summer, the soil gas diffusivity (Fig. 6) reaches its maximum value at the summit while it reaches its lowest value at the footslope. Soil gas diffusivity is ca. 10 times lower at the footslope relative to the summit.

Soil CO_2 concentrations (Fig. 6) are ca. 3 times lower at the summit relative to the footslope. Along soil profiles, soil CO_2 concentrations increases with depth, following a double exponential trend as described in Wiaux et al. (2014c).This second exponential curve begins at ca. 50 depth, and is especially pronounced at the footslope, reflecting a shift of ca. 4 % CO_2 between 44 and 100 cm depth. The time course of soil CO_2 concentrations at both the summit and the footslope increases from spring to late summer and then decreases to reach its lowest value in the late autumn.

The CO_2 fluxes (Fig. 6) were calculated based on both CO_2 concentrations and diffusivity following the method described in Wiaux et al. (2014c). These calculated CO_2 fluxes vary in the same range of values when comparing the footslope and the

BGD
11, 13699–13737, 2014

summit. However, the peaks do not occur at the same period from a slope position to another, with maximum CO_2 fluxes being emitted respectively during summer and autumn for the summit and the footslope. In addition, the duration of these maximum peaks differ between the summit and the footslope. Along the soil profiles, CO_2 fluxes decrease with depth and reach null values at ca. 30 cm depth at the summit and at ca. 15 cm depth at the footslope.

The distribution of the soil CO_2 fluxes in the profile is illustrated in Fig. 7. At the footslope, ca. 90 to ca. 95 % of the surface CO_2 fluxes is generated in the 10 first centimeters of the soil profile. The soil layer between 10 and 20 cm contribute for only 5 to 10 % depending of the period, and the deeper layers dot not significantly contribute to the surface fluxes. At the summit, the relative contribution of the different soil layers is more dynamic in time, with a contribution of the 10 first centimeters of the soil profile ranging from ca. 80 % at the late spring, decreasing to ca. 60 % in the early summer, and reaching ca. 40 % from late summer to the late autumn. At the summit, the 30 first centimeters of the soil profile significantly contribute to surface fluxes. This contribution decreases with depth in the late spring and the early summer, but is homogeneously distributed with depth for the rest of the time. At the summit, soil layers deeper than 30 cm depth sometimes contribute for up to 20 % of the total flux, especially in the autumn. Between 40 to 50 cm depth, and 80 to 90 cm depth, some negative contribution (i.e. CO_2 uptake) up to −20 % is also observed.

3.2 Modeling of surface CO_2 fluxes

Results of the daily aggregated simulation with the SoilCO_2-RothC model are summarized in Table 1 and Fig. 6. The simulated soil temperatures and VWC represent adequately the observations (Table 1). The simulated CO_2 fluxes fit well the CO_2 fluxes in 2013, both for the summit and the footslope. This fit is less good at the footslope ($R^2 = 42$ %, Table 1) but it remains acceptable given the quite local shift between observations and model simulations (Fig. 8). This shift (model underestimation) may be explained by the contribution of soil alkalinity to soil CO_2 fluxes during specific dry

BGD
11, 13699–13737, 2014

events in summer (e.g. Laponis et al., 2008). Punctual surface CO_2 fluxes measurements (Licor chamber system) extended to daily values corroborate the goodness of fit (GOF) of the simulations in 2012 (Table 1 and Figs. 6 and 7).

Simulated surface CO_2 fluxes (Fig. 8) remains more or less in the same range of values (from 0 to 6 g C m^{-2} day^{-1} in 2011 and 2013, and up to 8 g C m^{-2} day^{-1} in 2012). However, the temporal dynamic differs between slope positions and between years of simulation, with a clear alternation of peaks of year 2011 and 2013. At the summit, CO_2 fluxes increases from the winter to reach their maximum during the summer and then decreases again (Fig. 8), similarly to the temporal dynamic of soil temperature (see Fig. 5 as an exemple). At the footslope, the lowest CO_2 fluxes occur in the middle of the summer of each year, while a very high CO_2 fluxes can be observed from the late summer until the early autumn in 2011 and 2013 as well as in spring of year 2011 (Fig. 8).

The time integrated CO_2 fluxes are presented in Table 2. For the considered a simulation period of 3 years, the footslope emits ca. 1.5 more CO_2-C than the summit ($p < 0.01$), which represents an additional flux of 287 ± 106 g CO_2-C m^{-2} $year^{-1}$. The uncertainty on model simulations (given by ME values in Table 2) remains lower than the difference between slope positions for each year (Table 2). Once integrated at the hillslope scale, this means that such a loamy hillslope emit ca. 1.2 times more CO_2-C relative to a flat landscape ($p < 0.1$).

4 Discussion

4.1 Soil physical control on CO_2 emissions

The difference of the temporal dynamic of surface soil CO_2 fluxes between footslope and summit positions, as illustrated in Fig. 6, indicates that the limiting factors on flux emissions are not the same all along the hillslope. At the summit, on one hand, the dynamic of surface soil CO_2 fluxes clearly follows the temperature variations (Fig. 5,

BGD
11, 13699–13737, 2014

maximum during the summer). At the footslope, on the other hand, the surface soil CO_2 fluxes (Fig. 6) are small when the soil is close to water saturation. This is related to the fact that a high water filled pore space disables the transfer of biotic CO_2 along the soil profile (Fig. 1). The surface soil CO_2 flux dramatically increases when the gas diffusivity exceeds a threshold value of ca. 0.1 $cm^2\,d^{-1}$ (i.e. from day 255 to 305 of year 2013, Fig. 6).

In the period preceding this important CO_2 emission, the soil CO_2 cannot move along the soil profile and accumulates within soil pores. This results in a CO_2 concentration increase both in the early and the late summer, especially below ca. 50 cm depth (Fig. 5). This phenomenon is particularly evident below the compacted soil layer between ca. 40 and ca. 50 cm depth. This is consistent with the porosity profile described by Wiaux et al. (2014c) and illustrated in Fig. 2. This also corroborates the results of Wiaux et al. (2014c), suggesting that in downslope Colluvic Regosols, gas diffusion barriers (explained by a compacted soil layers) strongly impact the CO_2 concentration profile, and hence the temporal dynamic of resulting CO_2 flux at the soil surface. This supports recent studies (e.g. Ball, 2013) that showed that soil pore continuity and size are key to understand the mechanisms regulating the soil gases emissions.

As a consequence, the significantly higher CO_2 concentration at the footslope relative to the summit, especially in deep soil layers, is not explained by the large amount of soil labile OC along the footslope soil profile (Wiaux et al., 2014a, b) but is more likely the result of the accumulation along time (during too low diffusivity periods). Maier et al. (2011) showed that the CO_2 efflux can deviate from the instantaneous soil respiration due to CO_2 storage into soil pore spaces. Hence, soil physical variables are dominating the control of surface CO_2 fluxes at the footslope. This supports the conceptual improvement of the SOILCO$_2$-RothC model realized in this study, and the use of soil specific hydrodynamic parameters to characterize the gas diffusion (Moldrup et al., 2000).

Due to the interactions between variables and the complexity of the above-described system, simple correlation analyses will often not provide satisfactory results when

BGD
11, 13699–13737, 2014

studying soil respiration (Maier et al., 2011; Wiaux et al., 2014b), especially across sloping landscapes. This highlights the importance to use process-based C dynamic models considering both production and transfer terms (i.e. SoilCO_2-RothC) when studying the soil CO_2 efflux.

In summary, we highlight that the mechanisms which govern soil surface CO_2 emissions vary throughout the landscape. On a well-drained soil at the summit, observed soil CO_2 emissions are directly related to the CO_2 production through the phenomenon of soil micro-organisms respiration. However, on a wet footslope, observed temporal dynamic of soil CO_2 emissions much more reflects the physical transfer mechanisms: long periods of CO_2 production and accumulation alternate with periods of important release at the soil surface.

4.2 Soil organic carbon storage in downslope deposits

Soil respiration rate can be interpreted as an indicator of soil OC persistence (e.g. Gregorich et al., 1994). However, a further analysis of what occurs along the soil profile is needed to thoroughly answer the question of the persistence of OC. The vertical partitioning of the soil CO_2 fluxes, as illustrated in Fig. 7, shows that ca. 90 to ca. 95 % of the surface CO_2 fluxes originates from the 10 first centimeters of the soil profile at the footslope. Given the important amount of OC until up to 100 cm depth in our study site (Fig. 1, Wiaux et al., 2014a), this observation is not in agreement with the study of Goffin et al. (2014), who suggest that the relative contribution of the soil layers to the surface CO_2 fluxes is related to OC distribution along the soil profile. This higher contribution of the upper soil layers seems to be neither related to higher temperatures values (Fig. 5), contrary to what was suggested by Takahashi et al. (2004). According to the CO_2 concentration and diffusivity profiles (Fig. 6), the relative contribution of the soil layers to the surface CO_2 fluxes is more likely governed by soil physical controls (Ball, 2013) rather than by biological production depending on thermal energy and OC substrate. Here, soil gas diffusivity strongly decreases from 10 to 40 cm depth

BGD
11, 13699–13737, 2014

(where diffusivity is null) at the two slope positions, and the profile of CO_2 concentration displays no gradient between 10 and 40 cm depth specifically at the footslope (Fig. 6).

Here, we show that despite the low contribution of soil layers deeper than 10 cm depth (Fig. 7), the top soil layer (0–10 cm) generates CO_2 fluxes which exceed those observed at the summit position (Table 2), due to the major contribution (ca. 90 %) of the surfacing soil OC to the total CO_2 fluxes at the footslope position (Fig. 7). This can be explained by environmental conditions specific to this 0–10 cm layer playing in favor of both microbial respiration and gas diffusion. Indeed, close to the soil surface, both diffusion barriers and limitation of the access to the oxygen disappear. Hence, the only residual impact of soil VWC on soil respiration is its positive effect due to the increased access of soil micro-organisms to their OC substrate, and to the enhancement of their metabolic activities by water (Akinremi et al., 1999; Castellano et al., 2011; Herbst et al., 2008; Howard and Howard, 1993; Šimůnek and Suarez, 1993). The combination of this high amount and high quality of soil OC (Fig. 1, as described by Wiaux et al., 2014a) with this net positive effect of soil VWC results in a strong increase of microbial respiration rates.

Our results suggest that buried soil OC in colluvial deposits is stored for a long time below 10 cm depth, which corroborates the assumption of a long-term stabilization of deeply buried OC in downslope colluviums suggested in the literature (Doetterl et al., 2012; Berhe et al., 2008, 2012a). Hence, despite that deep soil OC (e.g. in colluvial deposits) has been shown to be highly processed (Rumpel and Kögel-Knabner, 2011), our results suggest that this OC turnover occurs in a closed soil sub-system that is potentially disconnected from the atmospheric C pool. This explains why the total and labile soil OC pools remain important and homogeneously distributed along the soil profile at the footslope, while it exponentially decreases with depth at the summit (Fig. 1, as described by Wiaux et al., 2014a).

Some studies suggest that net C sequestration occurs at the depositional sites (e.g. Smith et al. 2005), while others negate the apparent C sink caused by soil OC burial at depositional sites (e.g. Yoo et al. 2005). Here, our results reconcile two seemingly

BGD
11, 13699–13737, 2014

contradictory assertions: (i) buried soil OC at a footslope is efficiently stored in the subsoil and submitted to a long-term stabilization (Doetterl et al., 2012; Berhe et al., 2008, 2012a), and (ii) the footslope profile emits more CO_2 than the summit (Reicosky et al., 2005; Webster et al., 2008b; Wiaux et al., 2014b).

4.3 Quantification of soil-atmosphere CO_2 fluxes at the hillslope scale

Despite the fact that peaks of CO_2 fluxes are the highest at the summit position, cumulative CO_2 fluxes are the highest at the footslope position from year 2011 to 2013 (Fig. 8). As a consequence, the total annual flux averaged along 3 years of simulation is ca. 1.5 times higher ($p < 0.01$) at the footslope relative to the summit (Table 2). These observations are consistent with the results of Webster et al. (2008a, b) in forest fields, who observed 1.6 higher median respiration fluxes at footslope and toeslope positions compared to the crest and convex shoulder positions. These observations are also in agreement with the recent findings Wiaux et al. (2014b) based on punctual surface Licor chamber measurements on the same site, showing that mean respiration fluxes (standardized at 15 °C) were ca. 1.3 times higher at the footslope and 1.5 times higher at the toeslope ($p \leq 0.05$) relative to the summit position. The reason of this trend is that factors that control soil OC respiration are heterogeneously distributed across sloping landscapes (Reicosky et al., 2005; Webster et al., 2008b; Martin and Bolstad, 2009; Wiaux et al., 2014b).

Our estimations of annual CO_2 fluxes may be associated with large uncertainties due to error propagation on measured variables. Despite the modest performance of the SoilCO2-RothC model in reproducing the CO2 fluxes observation (R2 ranging between 42 and 64 %, Table 7.1), the model uncertainties (given by ME values, Table 7.2) are lower than the difference of annual CO_2 fluxes between slope positions (Table 7.2). In addition, this model error (sum of the difference between observations and simulations for each day of the year) observed in this study (from 4 to 91 g CO_2-C m^{-2} $year^{-1}$, Table 7.2) are lower than the uncertainty on the CO_2 fluxes directly measured at the catchment scale using the Eddy-covariance technique (from 100 to 200 g CO_2-C m^{-2} $year^{-1}$

BGD
11, 13699–13737, 2014

at non-ideal sites like sloping plots, Baldocchi, 2003). Hence, this supports the validity of the quantitative comparison of CO_2 fluxes between slope positions carried out in this study.

Focusing on CO_2 fluxes aggregated at the scale of the entire hillslope, such a loamy hillslope emits 683 ± 36 g CO_2-C m^{-2} $year^{-1}$ while a flat landscape would only emits 583 ± 61 g CO_2-C m^{-2} $year^{-1}$ (Table 2). For our study site, accounting only for soil C dynamics representative of flat landscapes would under-estimate annual soil-atmosphere CO_2 exchanges by ca. 20 %. This supports similar conclusions drawn under a forest eco-system by Webster et al. (2008a), who highlighted a risk of under- or over-estimation of soil respiration at large scale reaching up to 30 % when topography is not accounted for. Our results provide a thorough quantification and a better understanding of the soil-atmosphere C exchanges specific to an agro-ecosystem on the loess belt in Belgium, which may be of high importance to adopt strategies to mitigate climate change.

The CO_2 emissions values reported in literature studies as soil heterotrophic respiration (considering that heterotrophic respiration fluxes constitute ca. 30 % of the total ecosystem respiration and ca. 78 % of total soil respiration, according to Suleau et al., 2011) are ranging from ca. 170 to ca. 456 g CO_2-C m^{-2} $year^{-1}$ in similar conditions i.e. temperate loamy croplands (adapted from Boeckx et al., 2011; Kutsch et al., 2010; Paustian et al., 1990), from ca. 140 to ca. 144 g CO_2-C m^{-2} $year^{-1}$ in forests ecosystems (adapted from Dai et al., 2012; Webster et al., 2008a), and reach ca. 1811 g CO_2-C m^{-2} $year^{-1}$ in temperate grasslands on organic soils (adapted from Renou-Wilson et al., 2014). However, most of these studies were carried out on flat landscapes. To our knowledge, no equivalent quantification of the hillslope aggregated CO_2 fluxes already exists for agro-ecosystems. The values of CO_2 emissions presented in this study are in the same order of magnitude but are slightly higher than literature studies on flat croplands (Boeckx et al., 2011; Kutsch et al., 2010; Paustian et al., 1990). This may be explained by the hilly relief of this study site and the lateral transfer of soil particles en-

BGD
11, 13699–13737, 2014

riching the downslope area in soil OC (Wiaux et al., 2014a), inducing higher respiration rate relative to a flat uneroded position (Wiaux et al., 2014b).

The higher heterotrophic respiration at our study site compared to other temperate loamy croplands (Boeckx et al., 2011; Kutsch et al., 2010; Paustian et al., 1990) could also be explained by some experimental biases: (i) a priming effect due to the land-use change (soil kept bare and undisturbed during 3 years); (ii) any heading due to the dark geotextile installed at the surface of the measurements stations; and (iii) the modest model performances in terms of predictivity (Table 1). Hence, the absolute estimation of the hillslope aggregated CO_2 fluxes in this study should be interpreted carefully, and the focus should be on the relative difference between emissions from flat and sloping landscapes (i.e. 20 %, Table 2).

In order to understand the impact of these findings in terms of C balance, it is important to compare these heterotrophic respiration fluxes to other soil C inputs and outputs. Among other things, soil heterotrophic respiration fluxes discussed here only constitute ca. 30 % of the total ecosystem respiration, also composed of aboveground and belowground autotrophic respiration fluxes (Suleau et al., 2011) which were not considered here. However, this exceeds the scope of this study and should be explored at the scale of hillslopes in future researches.

Notwithstanding these elements, our results support that, when modeling soil C dynamics and when quantifying soil-atmosphere CO_2 exchanges, this is of paramount importance to consider slopes and elevation effects rather than a flat landscape, and to account for dynamic processes (e.g. lateral transfer of soil OC and heterogeneous distribution of soil VWC) occurring along hillslopes.

5 Conclusions

At the summit position of the studied hillslope, the time course of surface soil CO_2 fluxes clearly follows the time course of temperature (Figs. 5 and 6, maximum during the summer). At this position of the hillslope, observed soil CO_2 emissions are directly

BGD
11, 13699–13737, 2014

related to the CO_2 production through soil micro-organisms respiration. At the footslope, high water filled pore space disables the transfer of biotic CO_2 along the soil profile, and the surface soil CO_2 flux substantially increases when the gas diffusivity exceeds a given threshold value. Hence, on a wet footslope, the time course of observed soil CO_2 emissions is more determined by the physical transfer mechanisms: long periods of accumulation alternate with periods of important surface release. Considering these elements, the entire hillslope emits ca. 20 % more g CO_2-C m^{-2} $year^{-1}$ compared to a similar flat plot. This results support the need to consider slopes when modeling soil-atmosphere C exchanges.

The vertical partitioning of the soil CO_2 fluxes shows that ca. 90 to ca. 95 % of the surface CO_2 fluxes originates from the 10 first centimeters of the soil profile at the footslope. However, the total annual flux averaged along 3 years of simulation show that the top soil layer (0–10 cm) of the footslope generates CO_2 fluxes which exceed those observed at the summit position. Hence, our results reconcile two seemingly contradictory hypotheses, i.e. (i) these support that soil OC at such a footslope is stored along the main part of the soil profile and submitted to a long-term stabilization, and (ii) at the same time these support that the footslope profile emits more CO_2 than the summit.

Author contributions. F. Wiaux designed the experiments, carried them out, and performed the model simulations. M. Vanclooster, K. Van Oost, and F. Wiaux discussed the results and selected the messages to highlight. F. Wiaux wrote the main part of the paper and prepared the manuscript with contributions from all co-authors.

Acknowledgements. This study was funded by the Fonds National pour la Recherche Scientifique (FNRS, Belgium, convention no. 1.A306.12) and by the Fonds de la Recherche Fondamentale Collective (FRFC, convention no. 2.4590.12). F. Wiaux and K. Van Oost are supported by the FNRS. We thank the technician team of the UCL, especially F. Laurent for its precious help and ideas in establishing the experimental setup for in-situ soil CO_2 concentration profile measurements, and S. François for having achieved most of field campaigns of soil surface respiration measurements during more than 2 years. We kindly acknowledge J. Gillabel, from the Katholiek Universiteit van Leuven (Belgium), for its precious scientific and technical advices.

BGD
11, 13699–13737, 2014

The experimental design illsutrated on Fig. 4 has been inspired from which described in his PhD thesis (non peer-reviewed works). Last but not least, we thank Michael Herbst (Forschungszentrum Jülich, Institute of Bio- and Geosciences, Germany) for sharing and adapting the code of the SOILCO$_2$-RothC model, and for his precious assisstance and advices about the use of this model.

References

Akinremi, O., McGinn, S., and McLean, H.: Effects of soil temperature and moisture on soil respiration in barley and fallow plots, Can. J. Soil Sci., 79, 5–13, 1999.

Baldocchi, D. D.: Assessing the eddy covariance technique for evaluating carbon dioxide exchange rates of ecosystems: past, present and future, Glob. Change Biol., 9, 479–492, 2003.

Ball, B. C.: Soil structure and greenhouse gas emissions: A synthesis of 20 years of experimentation, Eur. J. Soil Sci., 64, 57–373, 2013.

Berhe, A. A., Harden, J. W., Torn, M. S., and Harte, J.: Linking soil organic matter dynamics and erosion-induced terrestrial carbon sequestration at different landform positions, J. Geophys. Res., 113, G04039, doi:10.1029/2008JG000751, 2008.

Berhe, A. A., Harden, J. W., Torn, M. S., Kleber, M., Burton, S. D., and Harte, J.: Persistence of soil organic matter in eroding versus depositional landform positions, J. Geophys. Res., 117, G02019, doi:10.1029/2011JG001790, 2012.

Berhe, A. A. and Kleber, M.: Erosion, deposition, and the persistence of soil organic matter: Mechanistic considerations and problems with terminology, Earth Surf. Proc. Land., 38, 908–912, 2013.

Boeckx, P., Van Nieuland, K., and Van Cleemput, O.: Short-term effect of tillage intensity on N_2O and CO_2 emissions, Agronomy Sust. Developm. 31, 453–461, 2011.

Campbell, G. S.: A Simple Method for Determining Unsaturated Conductivity From Moisture Retention Data, Soil Sci., 117, 311–314, 1974.

Castellano, M. J., Schmidt, J. P., Kaye, J. P., Walker, C., Graham, C. B., Lin, H., and Dell, C.: Hydrological controls on heterotrophic soil respiration across an agricultural landscape, Geoderma, 162, 273–280, 2011.

Chaopricha, N. T. and Marín-Spiotta, E.: Soil burial contributes to deep soil organic carbon storage, Soil Biol. Biochem., 69, 251–264, 2014.

BGD
11, 13699–13737, 2014

Dai, Z., Trettin, C. C., Li, C., Li, H., Sun, G., and Amatya, D. M.: Effect of assessment scale on spatial and temporal variations in CH_4, CO_2, and N_2O fluxes in a forested Wetland, Water Air Soil Poll., 223, 253–265, 2012.

Davidson, E. A., Savage, K., Verchot, L. V., and Navarro, R.: Minimizing artifacts and biases in chamber-based measurements of soil respiration, Agr. Forest Meteorol., 113, 21–37, 2002.

Davidson, E. A., Savage, K. E., Trumbore, S. E., and Borken, W.: Vertical partitioning of CO_2 production within a temperate forest soil, Glob. Change Biol., 12, 944–956, 2006.

Doetterl, S., Six, J., Van Wesemael, B., and Van Oost, K.: Carbon cycling in eroding landscapes: Geomorphic controls on soil organic C pool composition and C stabilization, Glob. Change Biol., 18, 2218–2232, 2012.

Epron, D., Bosc, A., Bonal, D., and Freycon, V.: Spatial variation of soil respiration across a topographic gradient in a tropical rain forest in French Guiana, J. Trop. Ecol., 22, 565–574, 2006.

Eswaran, H., Van Den Berg, E., and Reich, P.: Organic carbon in soils of the World, Soil Sci. Soc. Am. J., 57, 192–194, 1993.

Eugster, W., Moffat, A. M., Ceschia, E., Aubinet, M., Ammann, C., Osborne, B., Davis, P. A., Smith, P., Jacobs, C., Moors, E., Le Dantec, V., Béziat, P., Saunders, M., Jans, W., Grünwald, T., Rebmann, C., Kutsch, W. L., Czerný, R., Janouš, D., Moureaux, C., Dufranne, D., Carrara, A., Magliulo, V., Di Tommasi, P., Olesen, J. E., Schelde, K., Olioso, A., Bernhofer, C., Cellier, P., Larmanou, E., Loubet, B., Wattenbach, M., Marloie, O., Sanz, M.-J., Søgaard, H., Buchmann, N.: Management effects on European cropland respiration, Agr. Ecosys. Environ., 139, 346–362, 2010.

Gallagher, M. and Doherty, J.: Parameter estimation and uncertainty analysis for a watershed model, Environ. Modell. Softw., 22, 1000–1020, 2007.

Goffin, S., Aubinet, M., Maier, M., Plain, C., Schack-Kirchner, H., and Longdoz, B.: Characterization of the soil CO_2 production and its carbon isotope composition in forest soil layers using the flux-gradient approach, Agr. Forest Meteorol., 188, 45–57, 2014.

Goulden, M. L., Munger, J. W., Fan, S.-M., Daube, B. C., and Wofsy, S. C.: Measurements of carbon sequestration by long-term eddy covariance: methods and a critical evaluation of accuracy, Glob. Change Biol., 2, 169–182, 1996.

Gregorich, E. G., Carter, M. R., Angers, D. A., Monreal, C. M., and Ellert, B. H.: Towards a minimum data set to assess soil organic matter quality in agricultural soils, Can. J. Soil Sci., 74, 367–385, 1994.

BGD
11, 13699–13737, 2014

Herbst, M., Hellebrand, H. J., Bauer, J., Huisman, J. A., Simunek, J., Weihermuller, L., Graf, A., Vanderborght, J., and Vereecken, H.: Multiyear heterotrophic soil respiration: Evaluation of a coupled CO_2 transport and carbon turnover model, Ecol. Model., 214, 271–283, 2008.
Houghton, R. A.: Why are estimates of the terrestrial carbon balance so different?, Glob. Change Biol., 9, 500–509, 2003.
Howard, D. M. and Howard, P. J. A.: Relationships between CO_2 evolution, moisture content and temperature for a range of soil types, Soil Biol. Biochem., 25, 1537–1546, 1993.
IPCC: Detection of the greenhouse effect in the observations, Clim. Change: The IPCC Scientific Assessment, edited by: Wigley, T. M. L. and Barnett, T. P., 239–256, 1990.
IPCC: Clim. change: the supplementary report to the IPCC scientific assessment, edited by: Houghton, J. T. and Callander, B. A., Cambridge University Press, 1992.
Kutsch, W. L., Aubinet, M., Buchmann, N., Smith, P., Osborne, B., Eugster, W., Wattenbach, M., Schrumpf, M., Schulze, E. D., Tomelleri, E., Ceschia, E., Bernhofer, C., Béziat, P., Carrara, A., Di Tommasi, P., Grünwald, T., Jones, M., Magliulo, V., Marloie, O., Moureaux, C., Olioso, A., Sanz, M. J., Saunders, M., Søgaard, H., and Ziegler, W.: The net biome production of full crop rotations in Europe, Agriculture, Ecosystems & Environment, 139, 336–345, 2010.
Lal, R.: Soil erosion and the global carbon budget, Environ. Int., 29, 437–450, 2003.
Maier, M., Schack-Kirchner, H., Hildebrand, E. E., and Schindler, D.: Soil CO_2 efflux vs. soil respiration: Implications for flux models, Agr. Forest Meteorol., 151, 1723–1730, 2011.
Maier, M. and Schack-Kirchner, H.: Using the gradient method to determine soil gas flux: A review, Agr. Forest Meteorol., 192–193, 78-95, 2014.
Martin, J. G. and Bolstad, P. V.: Variation of soil respiration at three spatial scales: Components within measurements, intra-site variation and patterns on the landscape, Soil Biol. Biochem., 41, 530–543, 2009.
Moldrup, P., Olesen, T., Schjønning, P., Yamaguchi, T., and Rolston, D. E.: Predicting the gas diffusion coefficient in undisturbed soil from soil water characteristics, Soil Sci. Soc. Am. J., 64, 94–100, 2000.
Mualem, Y.: A new model for predicting the hydraulic conductivity of unsaturated porous media, Water Resour. Res., 12, 513–522, 1976.
Paustian, K., Andren, O., Clarholm, M., Hansson, A. C., Johansson, G., Lagerlof, J., Lindberg, T., Pettersson, R., Sohlenius, B.: Carbon and Nitrogen Budgets of Four Agro-Ecosystems With Annual and Perennial Crops, With and Without N Fertilization, J. Appl. Ecol., 27, 60–84, 1990.

BGD
11, 13699–13737, 2014

Peters, W., Krol, M. C., Van Der Werf, G. R., Houweling, S., Jones, C. D., Hughes, J., Schaefer, K., Masarie, K. A., Jacobson, A. R., Miller, J. B., Cho, C. H., Ramonet, M., Schmidt, M., Ciattaglia, L., Apadula, F., Heltai, D., Meinhardt, F., Di Sarra, A. G., Piacentino, S., Sferlazzo, D., Aalto, T., Hatakka, J., Ström, J., Haszpra, L., Meijer, H. A. J., Van Der Laan, S., Neubert, R. E. M., Jordan, A., Rodó, X., Morguí, J. A., Vermeulen, A. T., Popa, E., Rozanski, K., Zimnoch, M., Manning, A. C., Leuenberger, M., Uglietti, C., Dolman, A. J., Ciais, P., Heimann, M., Tans, P. P.: Seven years of recent European net terrestrial carbon dioxide exchange constrained by atmospheric observations, Glob. Change Biol., 16, 1317–1337, 2010.

Pingintha, N., Leclerc, M. Y., Beasley, J. P., Zhang, G., and Senthong, C.: Assessment of the soil CO_2 gradient method for soil CO_2 efflux measurements: Comparison of six models in the calculation of the relative gas diffusion coefficient, Tellus B, 62, 47–58, 2010.

Quinton, J. N., Govers, G., Van Oost, K., and Bardgett, R. D.: The impact of agricultural soil erosion on biogeochemical cycling, Nat. Geosci., 3, 311–314, 2010.

Reicosky, D. C., Lindstrom, M. J., Schumacher, T. E., Lobb, D. E., and Malo, D. D.: Tillage-induced CO_2 loss across an eroded landscape, Soil and Tillage Research, 81, 183–194, 2005.

Rommens, T., Verstraeten, G., Poesen, J., Govers, G., Van Rompaey, A., Peeters, I., and Lang, A.: Soil erosion and sediment deposition in the Belgian loess belt during the Holocene: Establishing a sediment budget for a small agricultural catchment, Holocene, 15, 1032–1043, 2005.

Rumpel, C. and Kögel-Knabner, I.: Deep soil organic matter – a key but poorly understood component of terrestrial C cycle, Plant Soil, 338, 143–158, 2011.

Šimůnek, J. and Suarez, D. L.: Modeling of carbon dioxide transport and production in soil: 1. Model development, Water Resour. Res., 29, 487–497, 1993.

Smith, S. V., Sleezer, R. O., Renwick, W. H., and Buddemeier, R. W.: Fates of Eroded Soil Organic Carbon: Mississippi Basin Case Study, Ecol. Appl., 15, 1929–1940, 2005.

Stallard, R. F.: Terrestrial sedimentation and the carbon cycle: Coupling weathering and erosion to carbon burial, Global Biogeochem. Cy., 12, 231–257, 1998.

Suleau, M., Moureaux, C., Dufranne, D., Buysse, P., Bodson, B., Destain, J.-P., Heinesch, B., Debacq, A., Aubinet, M.: Respiration of three Belgian crops: Partitioning of total ecosystem respiration in its heterotrophic, above- and below-ground autotrophic components, Agr. Forest Meteorol., 151, 633–643, 2011.

BGD
11, 13699–13737, 2014

Tang, J. W., Baldocchi, D. D., Qi, Y., and Xu, L. K.: Assessing soil CO_2 efflux using continuous measurements of CO_2 profiles in soils with small solid-state sensors, Agr. Forest Meteorol., 118, 207–220, 2003.
Takahashi, A., Hiyama, T., Takahashi, H. A., and Fukushima, Y.: Analytical estimation of the vertical distribution of CO_2 production within soil: application to a Japanese temperate forest, Agr. Forest Meteorol., 126, 223–235, 2004.
Topp, G. C., Davis, J. L., and Annan, A. P.: Electromagnetic determination of soil water content: Measurements in coaxial transmission lines, Water Resour. Res., 16, 574–582, 1980.
Trumbore, S. E. and Czimczik, C. I.: Geology – An uncertain future for soil carbon, Science, 321, 1455–1456, 2008.
Turcu, V. E., Jones, S. B., and Or, D.: Continuous soil carbon dioxide and oxygen measurements and estimation of gradient-based gaseous flux, Vadose Zone J., 4, 1161–1169, 2005.
Van Genuchten, M. T.: A Closed-form Equation for Predicting the Hydraulic Conductivity of Unsaturated Soils1, Soil Sci. Soc. Am. J., 44, 892–898, 1980.
Van Oost, K., Verstraeten, G., Doetterl, S., Notebaert, B., Wiaux, F., Broothaerts, N., and Six, J.: Legacy of human-induced C erosion and burial on soil-atmosphere C exchange, P. Natl. Acad. Sci. USA, 109, 19492–19497, 2012.
Wang, Z., Van Oost, K., Lang, A., Quine, T., Clymans, W., Merckx, R., Notebaert, B., and Govers, G.: The fate of buried organic carbon in colluvial soils: a long-term perspective, Biogeosciences, 11, 873–883, doi:10.5194/bg-11-873-2014, 2014.
Webster, K. L., Creed, I. F., Beall, F. D., and Bourbonnière, R. A.: Sensitivity of catchment – aggregated estimates of soil carbon dioxide efflux to topography under different climatic conditions, J. Geophys. Res.-Biogeosci., 113, G03040, doi:10.1029/2008JG000707, 2008a.
Webster, K. L., Creed, I. F., Bourbonniere, R. A., and Beall, F. D.: Controls on the heterogeneity of soil respiration in a tolerant hardwood forest, J. Geophys. Res.-Biogeosci., 113, G03018, doi:10.1029/2008JG000706, 2008b.
Wiaux, F., Cornelis, J. T., Cao, W., Vanclooster, M., and Van Oost, K.: Combined effect of geomorphic and pedogenic processes on the distribution of soil organic carbon quality along an eroding hillslope on loess soil, Geoderma, 216, 36–47, 2014a.
Wiaux, F., Vanclooster, M., Cornelis, J. T., and Van Oost, K.: Factors controlling soil organic carbon persistence along an eroding hillslope on the loess belt, Soil Biol. Biochem., 77, 187–196, 2014b.

BGD
11, 13699–13737, 2014

Wiaux, F., Van Oost, K., Mohammadi, M. H., and Vanclooster, M.: New insights in the calculation of soil carbon dioxide fluxes by means of the gradient method, Euro. J. Soil Sci., in review, 2014c.

Yoo, K., Amundson, R., Heimsath, A. M., and Dietrich, W. E.: Erosion of upland hillslope soil organic carbon: Coupling field measurements with a sediment transport model, Global Biogeochem. Cyc., 19, 1–17, 2005.

Young, S. L., Pierce, F. J., Streubel, J. D., and Collins, H. P.: Performance of solid-state sensors for continuous, real-time measurement of soil CO_2 concentrations, Agron. J., 101, 1417–1420, 2009.

BGD

11, 13699–13737, 2014

Table 1. Regression coefficient (R^2, %) as an indicator of the goodness of fit (GOF) between observations and simulations.

	VWC[a]		Temperature[a]		CO_2flux[b]	
	2012	2013	2012	2013	2012	2013
Summit	64	73	100	100	63	64
Footslope	82	89	99	100	61	42

[a] For VWC and temperature, the R^2 value is given as an indication representative of the 10 cm depth soil layer (but similar values are encountered all along the soil profile).

[b] For CO_2 fluxes, the observations compared to model simulations are punctual surface measurements with the Licor chamber system in 2011 (n = 8 days) and 2012 (n = 15 days), while it is continuous daily time-series of gradient-based fluxes in 2013 (n = 129 daysat the summit, and n = 137 days at the footslope). Data are not shown for 2011 (too low number of observations for CO_2 fluxes, no observation for the other variables).

BGD
11, 13699–13737, 2014

Table 2. Yearly simulated CO_2 flux [g C m^{-2} $year^{-1}$] at different slope positions.

	Summit	Footslope	Diff.	Hillslope
2011 (± ME)	545 (−22)	944 (+26)	399 (+4)	685
2012 (± ME)	654 (+136)	842 (+63)	188 (−73)	719
2013 (± ME)	553 (+47)	826 (+138)	274 (+91)	647
Average ± SD	583 ± 61a***	870 ± 64b***	287 ± 106	684 ± 36c*

Note: Diff. is the difference between the footslope and the sumit yearly CO_2 flux.
Note: ME is the model error (sum of the difference between observations and simulations for each day of the year). A positive value means that model underestimates the flux, and inversely.
Note: SD is standard deviation. Mean values with different letters are significantly different from each other (Student test, *:$0.05 < p < 0.1$; **:$p < 0.05$; ***:$p < 0.01$). To calculate mean yearly CO_2 fluxes representative of a hilly landscape (hillslope), we achieved a weighted sum of the summit and the footslope fluxes, according to the fact that the footslope colluvium covers ca. 35 % of the surface of the studied hillslope.

BGD
11, 13699–13737, 2014

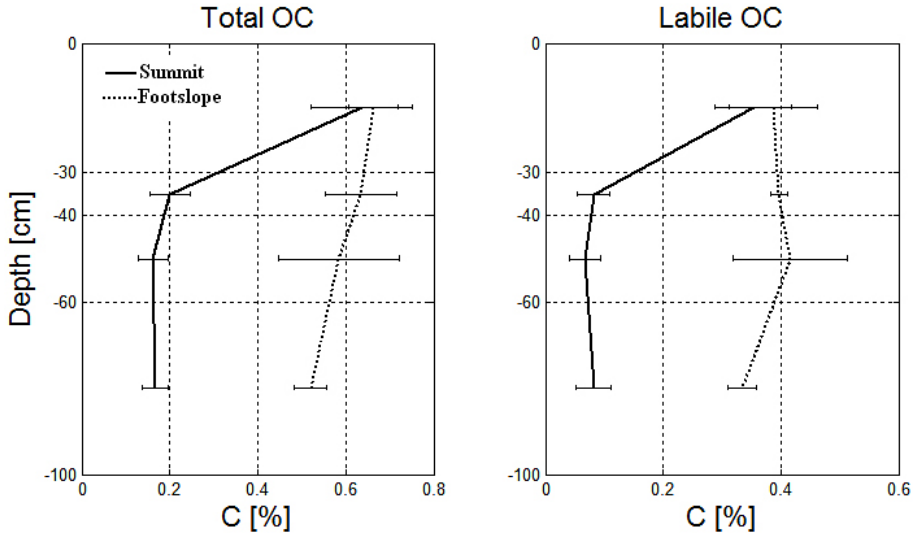

Figure 1. Soil profiles (0–100 cm) of both soil total OC and labile OC pool concentrations [C %], at the summit and footslope positions. Error bars indicate 1 standarddeviation ($n \leq 3$).

BGD
11, 13699–13737, 2014

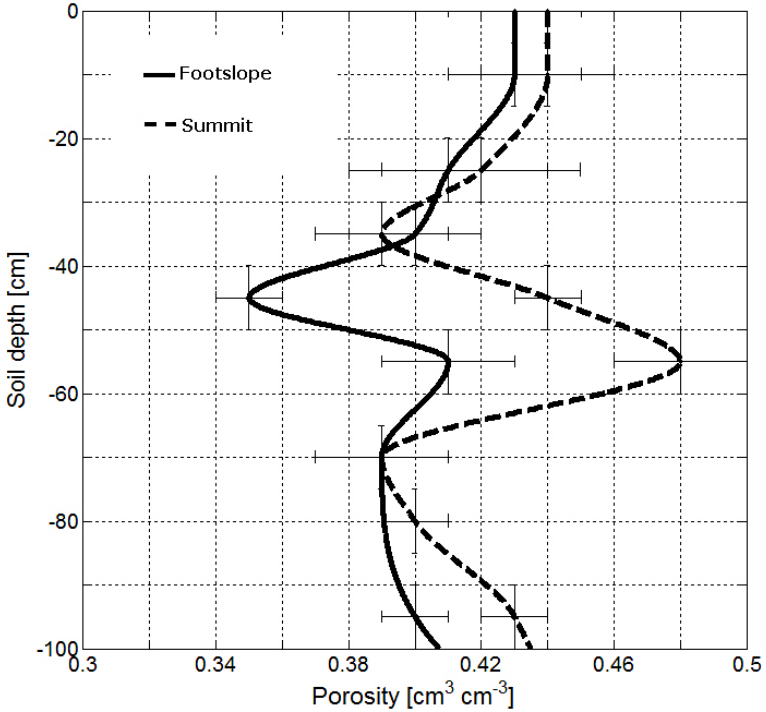

Figure 2. Soil porosity profiles at the footslope (plain line) and at the summit (dashed line) positions. Error bars indicate 1 standard deviation ($n \leq 3$). Continuous lines are linearly interpolated values.

BGD
11, 13699–13737, 2014

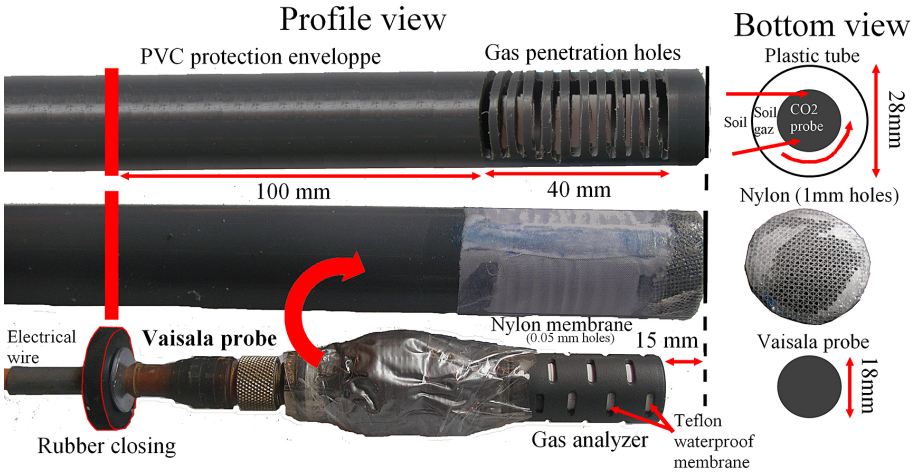

Figure 3. Description of the probes used for CO_2 concentration measurements inside the soil.

BGD
11, 13699–13737, 2014

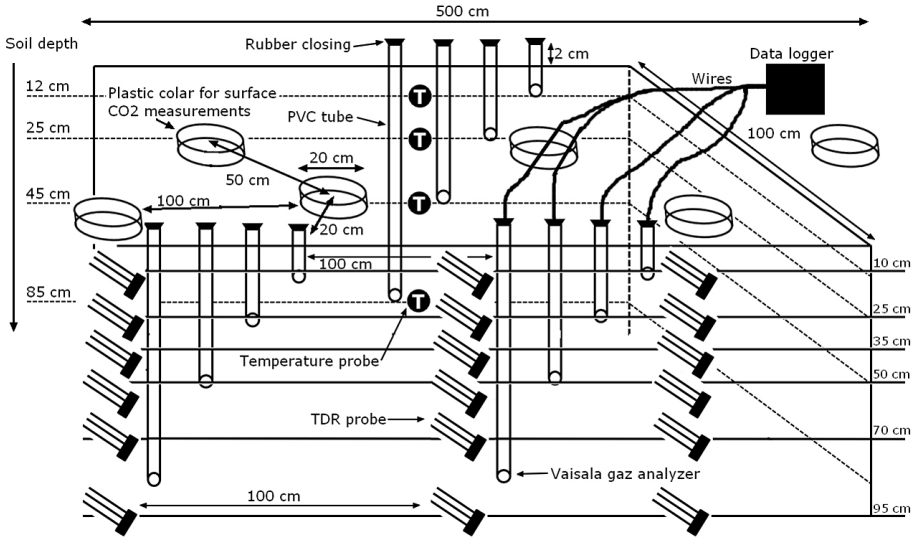

Figure 4. Schematic description of the experimental plot (sampling design) at each slope position.

BGD
11, 13699–13737, 2014

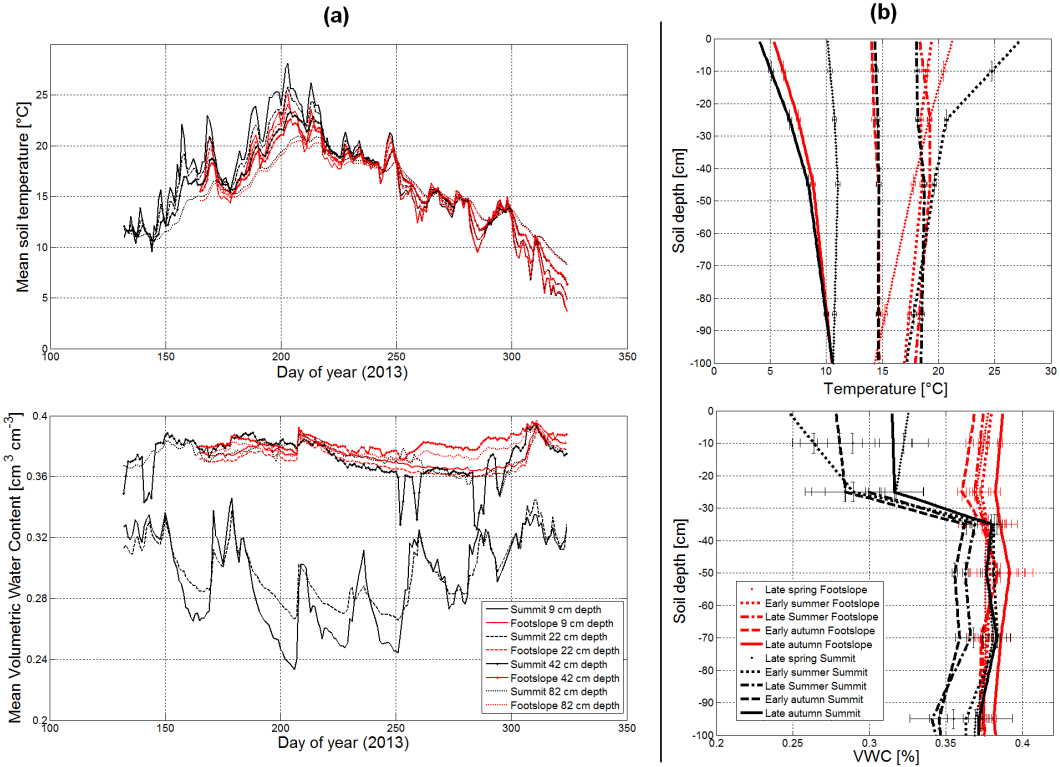

Figure 5. Space-time dynamic of soil temperature and moisture at the summit (red) and the footslope (black) position in 2013: **(a)** time series at different depths; **(b)** profile at different dates.

BGD
11, 13699–13737, 2014

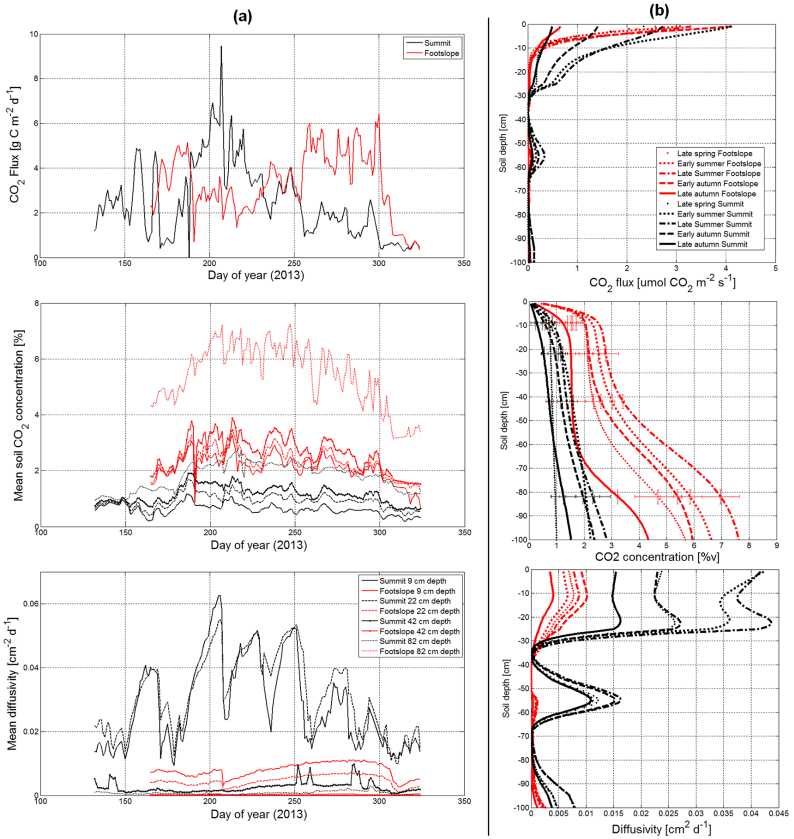

Figure 6. Space-time dynamic of soil CO_2 diffusivity, concentrations and fluxes at the summit (red) and the footslope (black) position in 2013: **(a)** time series at differ ent depths; **(b)** profile at different dates.

BGD
11, 13699–13737, 2014

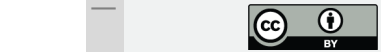

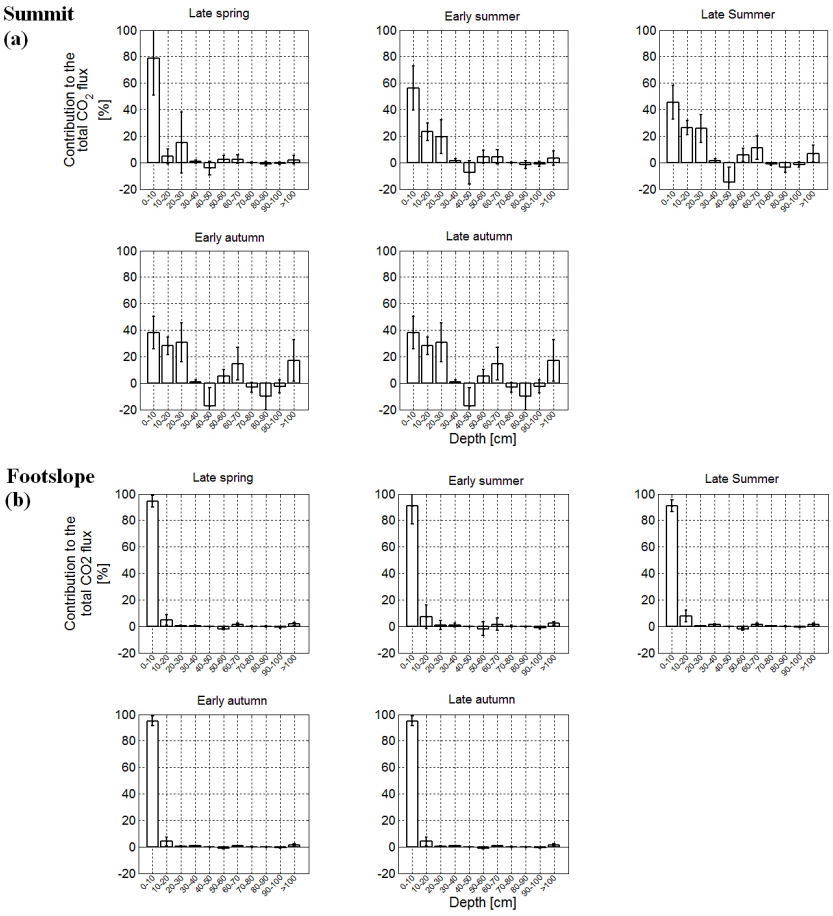

Figure 7. Depth distribution of the relative contribution to soilsurface CO_2 fluxes in year 2013 averaged by semi-seasons (error bars represent the standard deviation of the time aggregation for each soil layer): **(a)** at the summit, and **(b)** at the footslope position.

BGD
11, 13699–13737, 2014

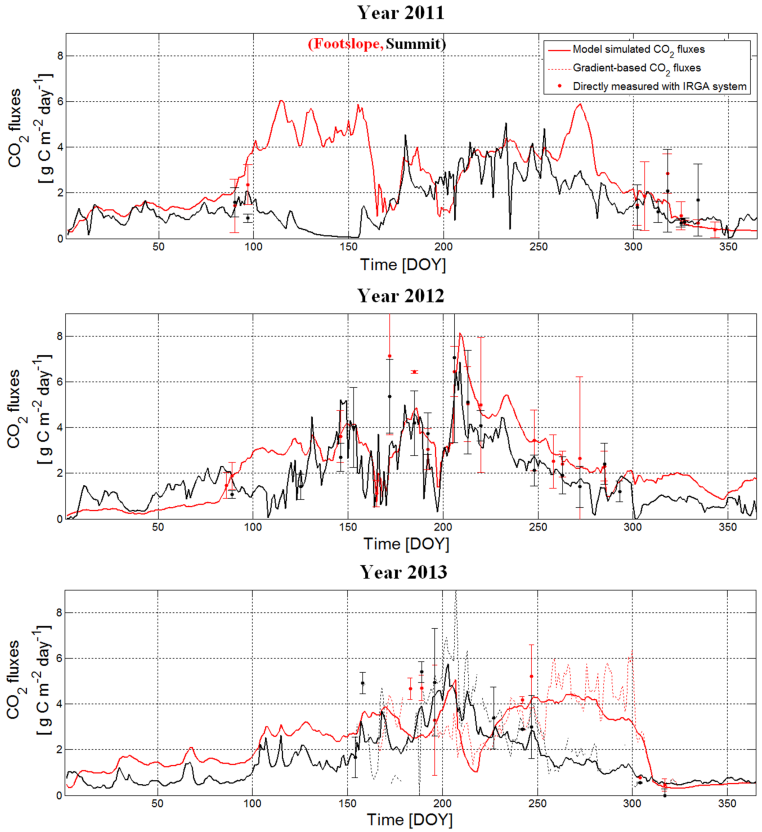

Figure 8. CO_2 fluxes from 2011 to 2013 at two slope positions (footslope in red, summit in black): **(i)** simulation based on the SOILCO$_2$-RothC model (plain lines), **(ii)** calculated fluxes with the gradient-based method (dashed lines), and **(iii)** spatial average of in situ measured fluxes with the IRGA Licor chamber (points with errorbars).

BGD
11, 13699–13737, 2014